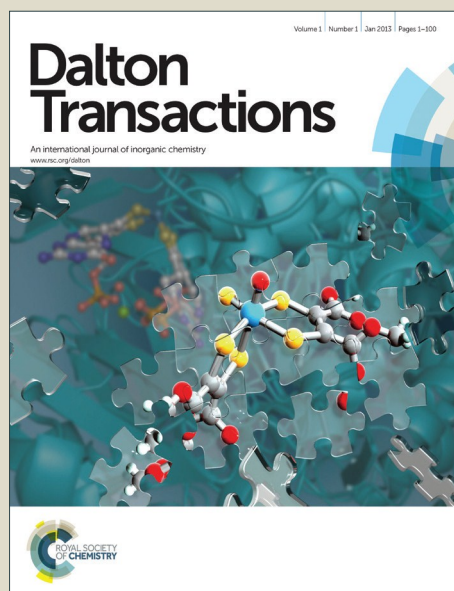


# Dalton Transactions

Accepted Manuscript



This article can be cited before page numbers have been issued, to do this please use: J. Jia, M. Cui, J. Dai and B. Liu, *Dalton Trans.*, 2015, DOI: 10.1039/C5DT00023H.



This is an *Accepted Manuscript*, which has been through the Royal Society of Chemistry peer review process and has been accepted for publication.

*Accepted Manuscripts* are published online shortly after acceptance, before technical editing, formatting and proof reading. Using this free service, authors can make their results available to the community, in citable form, before we publish the edited article. We will replace this *Accepted Manuscript* with the edited and formatted *Advance Article* as soon as it is available.

You can find more information about *Accepted Manuscripts* in the [Information for Authors](#).

Please note that technical editing may introduce minor changes to the text and/or graphics, which may alter content. The journal's standard [Terms & Conditions](#) and the [Ethical guidelines](#) still apply. In no event shall the Royal Society of Chemistry be held responsible for any errors or omissions in this *Accepted Manuscript* or any consequences arising from the use of any information it contains.

## ARTICLE

## 2-Phenylbenzothiazole Conjugated with Cyclopentadienyl Tricarbonyl [CpM(CO)<sub>3</sub>] (M = Re, <sup>99m</sup>Tc) Complexes as Potential Imaging Probes for $\beta$ -Amyloid Plaques

Cite this: DOI: 10.1039/x0xx00000x

Received 00th January 2012,  
Accepted 00th January 2012

DOI: 10.1039/x0xx00000x

www.rsc.org/

Jianhua Jia<sup>a</sup>, Mengchao Cui<sup>a,\*</sup>, Jiawei Dai<sup>b</sup> and Boli Liu<sup>a</sup>

Techneium-99m-labeled cyclopentadienyl tricarbonyl complexes conjugated with the 2-phenylbenzothiazole binding motif were synthesized. The rhenium surrogates **20**, **21**, **22** and **23** were demonstrated to have moderate to high affinities for A $\beta$ <sub>1-42</sub> aggregates with *K<sub>i</sub>* values of 142, 76, 64 and 24 nM, respectively. During the fluorescent staining of brain sections of transgenic mice and patients with Alzheimer's disease, these rhenium complexes demonstrated perfect and intense labeling of A $\beta$  plaques. Moreover, in *in vitro* autoradiography, <sup>99m</sup>Tc-labeled complexes clearly detected  $\beta$ -amyloid plaques on sections of brain tissue from transgenic mice, which confirmed the sufficient affinity of these tracers for A $\beta$  plaques. However, these compounds did not show desirable property *in vivo*, especially the poor brain uptake (below 0.5% ID/g), which hindered the further development of these tracers as brain imaging agents. Nonetheless, it is encouraging that these <sup>99m</sup>Tc-labeled complexes designed by conjugate approach displayed sufficient affinities for A $\beta$  plaques.

### Introduction

Alzheimer's disease (AD) is a progressive neurodegenerative disorder that leads to irreversible cognitive decline, memory impairment and behavioral changes.<sup>1, 2</sup> According to the World Health Organization, AD affects over 36 million people worldwide and will increasingly burden families and society with the ageing society deepening. Autopsied brains of AD patients have shown that senile plaques, composed of  $\beta$ -amyloid (A $\beta$ ) peptides, and neurofibrillary tangles (NFTs), consisting of highly hyperphosphorylated tau proteins, are the two main neuropathological features of AD.<sup>3, 4</sup> Based on targeting the two types of abnormal proteins, some new methods for the non-invasive diagnosis of early stage AD have been explored. Among them, the detection of A $\beta$  plaques *in vivo* by positron emission tomography (PET) has obtained some success. Based on the structures of Congo Red and Thioflavin-T, many <sup>11</sup>C- and <sup>18</sup>F-labeled imaging probes have been investigated, such as the PET imaging agents [<sup>18</sup>F]AV-45<sup>5</sup>,

[<sup>18</sup>F]GE067,<sup>6, 8</sup> and [<sup>18</sup>F]BAY-94-9172<sup>9, 10</sup>, which have been recently approved by FDA. However, these probes have disadvantages such as their relatively short half-lives, complicated synthetic manipulations, intense reliance on the cyclotron and expensive cost. <sup>99m</sup>Tc-labeled A $\beta$  probes for single photon emission tomography (SPECT) could, given the easier accessibility of <sup>99m</sup>Tc and its longer half-life compared to <sup>18</sup>F, provide a more convenient approach for the detection of AD. In the past few decades, some small and neutral <sup>99m</sup>Tc-labeled probes for A $\beta$  have been reported including derivatives of benzothiazole<sup>11-14</sup>, biphenyl<sup>15</sup>, flavone<sup>16, 17</sup>, chalcone<sup>18, 19</sup>, benzofuran<sup>20</sup> and so on. Among them, <sup>99m</sup>Tc-labeled 2-phenylbenzothiazole derivatives (Thioflavin-T skeleton structure) seemed to be very attractive. Several <sup>99m</sup>Tc chelation ligands, such as bis-amino-bis-thiol (BAT)<sup>11</sup>, monoamide monoamine (MAMA)<sup>11</sup>, hydrazino nicotinic acid (HYNIC)<sup>12</sup>, mercaptoacetyltriglycine (MAG3)<sup>12</sup>, iminodiacetic acid (IDA)<sup>12</sup>, picolylamine monoacetic acid (PAMA)<sup>13</sup> and bis(pyridin-2-ylmethyl)amine (DPA)<sup>14</sup>, were adopted in the 2-phenylbenzothiazole derivatives (Figure 1). However, most

## ARTICLE

of these  $^{99m}\text{Tc}$ -labeled probes displayed unfavorable binding affinities to the  $A\beta$  plaques and limited blood brain barrier (BBB) penetration; therefore, identifying a proper chelating ligand that can not only retain a high affinity for the  $A\beta$  plaques but also possess good brain penetration is pivotal in the design of  $^{99m}\text{Tc}$ -labeled brain imaging agents.

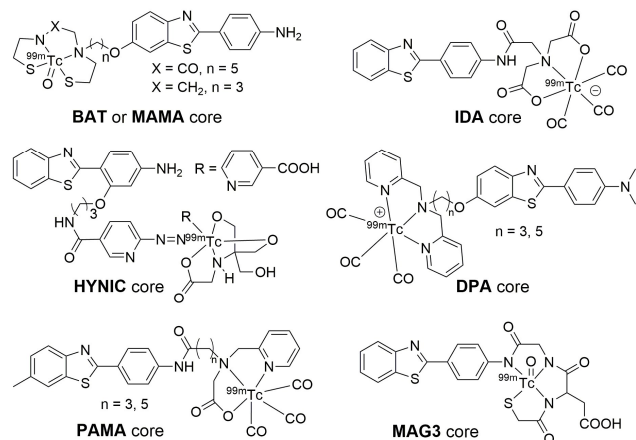


**Figure 1.** Chemical structures of the  $^{99m}\text{Tc}$ -labeled 2-phenylbenzothiazole derivatives previously reported as  $A\beta$  imaging probes.

Cyclopentadiene organometallic complexes, as versatile and typical entities, have been widely applied in radiometal-labeled tracers, and cyclopentadiene was considered to be an ideal candidate to stabilize complexes with the  $fac\text{-}[\text{M}(\text{CO})_3]^+$  ( $\text{M} = \text{Re}, ^{99m}\text{Tc}$ ) core.<sup>21</sup> The cyclopentadienyl tricarbonyl ligand ( $[\text{CpM}(\text{CO})_3]$ ) has inherent advantages, including its low molecular weight, moderate lipophilicity, small size, high stability of the half-sandwich configuration and minimal steric hindrance.  $[\text{CpM}(\text{CO})_3]$  could conjugate with the target molecule through different carbon linkers directly or mimic an aromatic group in relevant molecules. In summary,  $[\text{Cp}^{99m}\text{Tc}(\text{CO})_3]$  is considered to be a promising ligand for the design of  $^{99m}\text{Tc}$ -labeled brain receptor imaging agents. M. Saidi et al reported the complexes  $\text{M}(\text{CO})_3\text{Cp-COOC}_5\text{H}_9\text{N-R}$  ( $\text{M} = ^{99m}\text{Tc}, \text{Re}; \text{R} = \text{Me}, \text{isopropyl}$ ) for the *in vivo* imaging of serotonin 5-HT<sub>1A</sub> receptors in the brain, and they displayed significant affinities for the target receptor as well as high brain uptakes (1.02% ID/g) in rats 20 min after *i.v.* application.<sup>22</sup> Our group has recently described three  $^{99m}\text{Tc}$ -labeled cyclopentadienyl tricarbonyl complexes mimicking the chalcone structure for  $A\beta$  plaques in the brain by an integrated approach. The initial brain uptakes improved significantly ( $4.10 \pm 0.38\%$  ID/g for the  $^{99m}\text{Tc}$  complex with  $n = 1$ ), while the binding affinity for  $A\beta$  was not well retained by this integrated approach.<sup>18</sup> In general, a conjugate approach has an advantage in the binding

affinity compared with an integrated approach. In the present study, we reported the synthesis and evaluation of 2-phenylbenzothiazole derivatives conjugated with  $[\text{CpM}(\text{CO})_3]$  ( $\text{M} = ^{99m}\text{Tc}, \text{Re}$ ) by different carbon linkers (Figure 2).

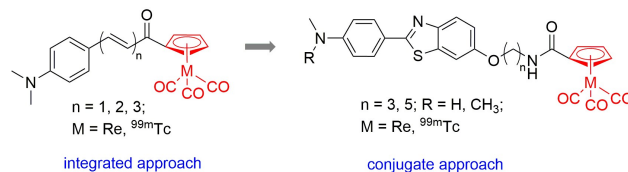


**Figure 2.** Chemical structures of  $[\text{CpM}(\text{CO})_3]$  ( $\text{M} = \text{Re}, ^{99m}\text{Tc}$ ) complexes mimicking chalcone and conjugated with 2-phenylbenzothiazoles.

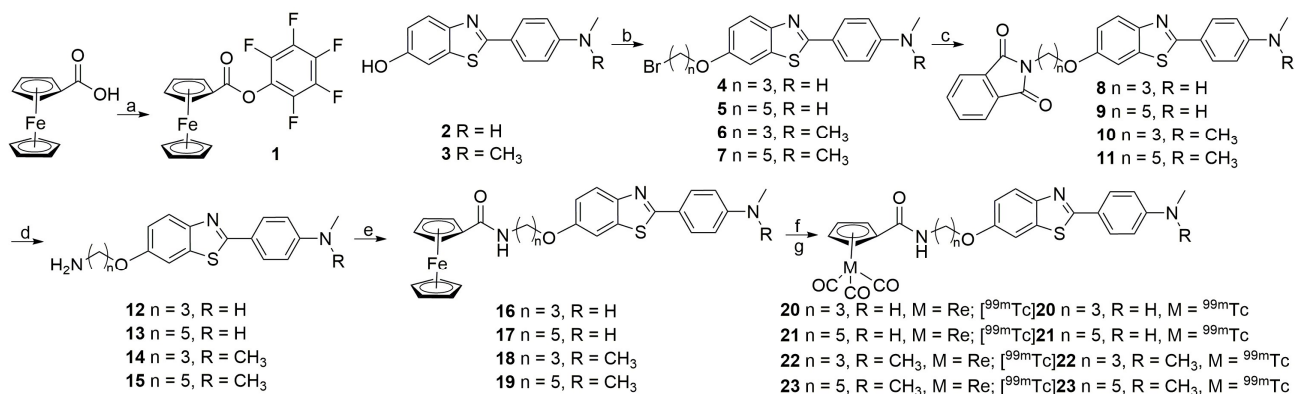
## Results and Discussion

### Chemistry

The synthetic route of the ferrocene precursors and corresponding rhenium complexes is shown in Scheme 1. The binding motifs of 2-phenyl benzothiazole hydroxyl compounds (**2** and **3**) and brominated compounds (**4**, **5**, **6** and **7**) were prepared as previously reported in the literature.<sup>14</sup> The primary amines **12**, **13**, **14** and **15** were obtained with acceptable yields though a Gabriel reaction by the hydrazinolysis of the corresponding N-alkylphthalimides (**8**, **9**, **10** and **11**). The ferrocene precursors **16**, **17**, **18** and **19** with different lengths of carbon linkers were synthesized through a condensation reaction from the active ferrocene ester and the primary amines **12**, **13**, **14** and **15**. Rhenium complexes **20**, **21**, **22** and **23**, as non-radioactive surrogates of the  $^{99m}\text{Tc}$ -labeled tracers, were obtained from the ferrocene precursors and  $(\text{NEt}_4)_2[\text{Re}(\text{CO})_3\text{Br}_3]$  at high temperature and high pressure in an autoclave with yields of approximately 20%. All of these complexes were fully characterized by spectroscopic methods. In addition, complex **23** could be recrystallized to produce X-ray quality crystals by slow evaporation of a mixed methanol and methylene dichloride solution. The ORTEP structure is illustrated in Figure 3, and the relevant crystallographic data are shown in Table 1. Complex **23** crystallizes in the triclinic space group  $P\bar{1}$ . The asymmetric unit contains one neutral complex and one methylene dichloride solvent molecule. The central rhenium atom is  $\eta^5$ -coordinated to the cyclopentadienyl ring, and the coordination sphere is completed by three carbonyl groups. The geometry around rhenium is pseudo-octahedral with average Re-Cp carbon bond lengths of 2.30 Å, Re-CO carbon bond lengths of 1.92 Å and C-Re-C (between CO) carbon bond angles of approximately 90°. The target molecule 2-phenylbenzothiazole skeleton retains a

planar structure and forms a certain angle with the Cp plane. The distance between the chelating group and the target molecule

decreases the spatial steric hindrance, therefore, the affinity of the target molecule is not expected to be greatly affected.

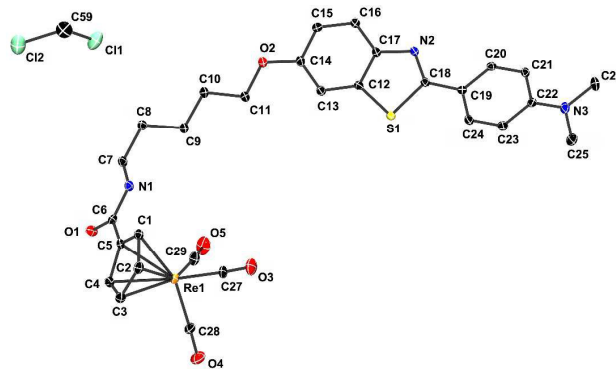


**Scheme 1.** Synthesis of Re/<sup>99m</sup>Tc-labeled 2-phenylbenzothiazoles. Reagents and conditions: a. perfluorophenyl 2,2,2-trifluoroacetate, pyridine, DMF, r.t., 3 h; b. 1,3-dibromo propane or 1,5-dibromo pentane, K<sub>2</sub>CO<sub>3</sub>, CH<sub>3</sub>CN, 90 °C, 4 h; c. potassium phthalimide, DMF, 100 °C, overnight; d. hydrazine hydrate, EtOH, 100 °C, 2 h; e. **1**, triethylamine, DMF, r.t., 4 h; f. [Re(CO)<sub>3</sub>Cl<sub>3</sub>][NEt<sub>4</sub>]<sub>2</sub>, HCl (1 M), DMF, 160 °C, 2 h; g. Mn(CO)<sub>5</sub>Br, Na[<sup>99m</sup>TcO<sub>4</sub>], H<sub>2</sub>O, DMF, 150 °C, 50 min.

**Table 1.** Summary of the X-ray crystallographic data for complex **23**.

Formula sum	C <sub>29</sub> H <sub>29</sub> N <sub>3</sub> O <sub>5</sub> SRe·CH <sub>2</sub> Cl <sub>2</sub>
M (g/mol)	801.74 g/mol
Crystal system	triclinic
Space-group	<i>P</i> -1
Cell parameters	a=7.8257(13) Å α=100.46(0)° b=13.264(2) Å β=90.16(0)° c=15.137(3) Å γ=101.81(0)°
Cell ratio	a/b=0.5900; b/c=0.8763; c/a=1.9343
Cell volume (Å <sup>3</sup> )	1511.15(119) Å <sup>3</sup>
Z	4
Calc. density (g/cm <sup>3</sup> )	1.76189 g/cm <sup>3</sup>
RAll	0.0521
Pearson code	aP144
Formula type	NOP3Q5R30...
Wyckoff sequence	i72

**Figure 3.** Crystal structure of complex **23** with the thermal ellipsoids drawn at the 30% probability level.



### Radiolabeling

The formation of <sup>99m</sup>Tc-labeled cyclopentadienyl tricarbonyl complexes is also depicted in Scheme 1, which is referred to as a double ligand transfer (DLT) reaction from ferrocene precursors according to the previously reported literature.<sup>23</sup> The <sup>99m</sup>Tc-labeled products were obtained under heat at 150 °C for 50 min with an average radiochemical yield of 50% (no decay correction), and the final pure <sup>99m</sup>Tc-labeled products (RCP > 98%, Figure 4 and Table S1) were obtained by purification with RP-HPLC. To identify the radioactive products, the retention times were compared between the non-radioactive rhenium surrogates and <sup>99m</sup>Tc-labeled radiotracers through co-injection and co-elution. Each pair of retention times differed by less than 1.5 min, which was in accordance with the time delay caused by the distance between the UV and radioactivity detectors.

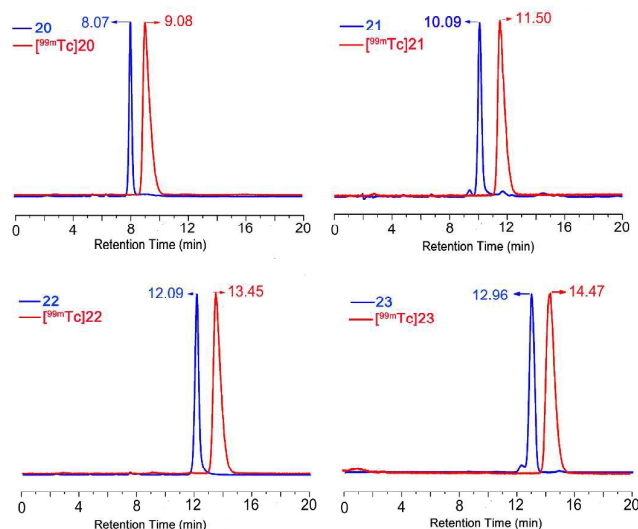


**Figure 4.** HPLC profiles of the purified complexes (blue lines, UV signals of the rhenium complexes; red lines, radioactivity signals of the  $^{99m}\text{Tc}$  complexes). HPLC conditions: Venusil MP C18 column (Agela Technologies, 4.6 mm  $\times$  250 mm),  $\text{CH}_3\text{CN}/\text{H}_2\text{O} = 80/20$ , 1 mL/min, UV, 254 nm.

### Biological Evaluation

**In Vitro Fluorescent Staining** The rhenium complexes displayed fluorescence emission properties in solution because of the conjugated 2-phenylbenzothiazole structure. The spectroscopic properties were shown in Table 2. Thus, neuropathological fluorescent staining experiments with rhenium complexes were implemented on sections of brain tissue from Tg mice (C57BL6, APP<sup>swe</sup>/PSEN1, 12-month-old, female) and an AD patient (91-year-old, male, temporal lobe) to confirm the affinity of the rhenium complexes for  $A\beta$  plaques. As shown in Figure 5, they specifically stained  $A\beta$  plaques on the brain sections of Tg mice (A, E, I and M), and the results were in agreement with the staining of adjacent brain sections (B, F, J and N) using Thioflavin-S (a histological dye for the clinical detection of  $A\beta$  plaques). As expected, there was not notable staining on the brain sections from normal mice with rhenium complexes (C, G, K and O) as well as with Thioflavin-S (D, H, L and P). Moreover, the  $A\beta$  plaques on the brain sections of the AD patient were clearly labeled by these compounds (Figure 6, A, B, C and D). More interestingly, NFTs and cerebrovascular amyloids on the brain sections of the AD patient (Figure 6, E and F, complex 23) could also be stained by these rhenium complexes, which indicated that they have affinities for tangles and cerebrovascular amyloids. The staining results demonstrated that these rhenium

complexes have affinities for  $A\beta$  plaques. Technetium and rhenium in the same group tend to have a shared chemistry, as well as similar structure and properties, therefore,  $^{99m}\text{Tc}$ -labeled complexes were predicted to also have affinities for  $A\beta$  plaques.

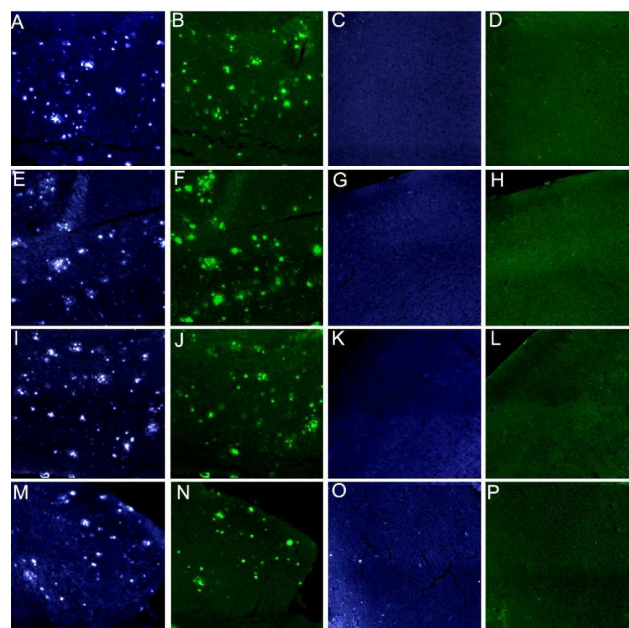


**Figure 5.** Fluorescent staining with **20** (A), **21** (E), **22** (I) and **23** (M) on the brain slices of Tg mice (C57BL6, APP<sup>swe</sup>/PSEN1, 12-month-old, female) and wild control mice (C57BL6, 12-month-old, female) (C, G, K and O). Adjacent sections were stained with Thioflavin-S for comparison (B, F, J and N) (D, H, L and P). (magnification: 5 $\times$ , DAPI filter, EX 365 nm, EM 445 nm)

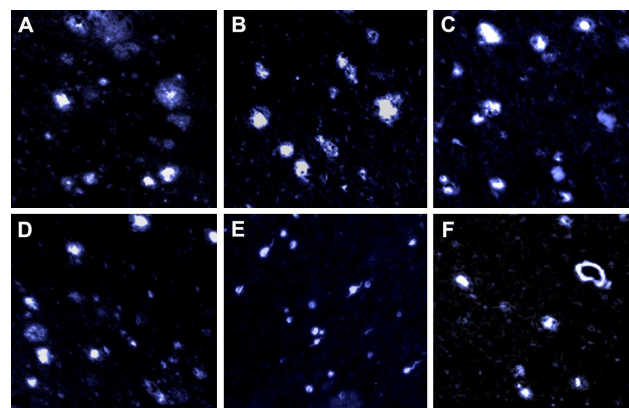


**Figure 6.** Fluorescent staining of **20** (A), **21** (B), **22** (C) and **23** (D, E and F) on the brain slices of an AD patient (91-year-old, male, temporal lobe). NFTs (E) and cerebrovascular amyloids (F) were also stained by **23**. (magnification: 10 $\times$ , DAPI filter, EX 365 nm, EM 445 nm)

**In Vitro Inhibition Assay** Competitive binding assays were performed to evaluate the affinity of these rhenium complexes for  $A\beta_{1-42}$  aggregates using 6- $[^{125}\text{I}]$ iodo-2-(4'-N,N-dimethylamino)phenylimidazo[1,2-a]-pyridine ( $[^{125}\text{I}]$ IMPY) as the competing radioligand. The binding of  $[^{125}\text{I}]$ IMPY to  $A\beta_{1-42}$  aggregates was inhibited by these rhenium complexes in a dose-dependent manner, which manifested their affinities for  $A\beta_{1-42}$  aggregates (Figure 7). As shown in Table 2, rhenium complexes showed moderate to high binding affinities for  $A\beta_{1-42}$  aggregates ( $K_i = 24.0 - 142.6$  nM). Complex **23**, with a N,N-dimethylamino group and longer carbon linker, displayed the highest affinity compared with the other three complexes. As shown in the crystal structure, although the entire molecule is not in a planar configuration, the affinity of the target molecule was well-retained due to the action of the carbon linker. The secondary N-methylamino analogues were found to have weaker affinities than the tertiary N,N-dimethylamino analogues (**20** vs. **22**, **21** vs. **23**), and the relatively longer carbon linker is beneficial for retaining the high affinities of the target molecules (**20** vs. **21**, **22** vs. **23**), which were similar to the rules previously reported.<sup>24</sup> Compared to the reported  $^{99\text{m}}\text{Tc}$ -labeled 2-phenylbenzothiazole analogues with other chelating groups, the  $^{99\text{m}}\text{Tc}$ -labeled cyclopentadienyl tricarbonyl benzothiazole analogues based on the conjugate approach displayed slightly higher affinities ( $K_i = 29.5 - 617$  nM)<sup>25</sup>. In addition, they possessed better affinities than the  $[\text{CpRe}(\text{CO})_3]$  complexes mimicking the chalcone structure, which were designed according to the integrated approach ( $K_i = 108 - 899$  nM)<sup>18</sup>. Additionally, the affinity of cold IMPY was also evaluated using the same assay conditions for comparison, and complex **23** displayed a comparable affinity to that of IMPY ( $K_i = 12.5 \pm 2.8$  nM).

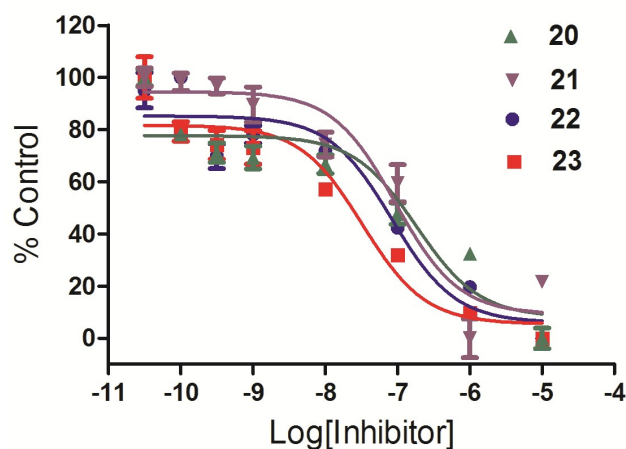


**Figure 7.** Inhibition curves of rhenium complexes for the binding of  $[^{125}\text{I}]$ IMPY to  $A\beta_{1-42}$  aggregates.

**Table 2.** The binding data and spectroscopic properties (absorption, excitation and emission wavelength) of rhenium complexes **20 – 23**.

Compound	$K_i$ (nM) <sup>a</sup>	abs (nm) <sup>b</sup>	$\lambda_{\text{ex}} / \lambda_{\text{em}}$ (nm) <sup>b</sup>
<b>20</b>	142.6 ± 25.9	360.2	364.0 / 421.0
<b>21</b>	75.8 ± 36.3	354.2	364.0 / 421.0
<b>22</b>	64.1 ± 13.9	356.4	364.0 / 424.0
<b>23</b>	24.0 ± 8.1	356.2	367.0 / 425.0
<b>IMPY</b>	12.5 ± 2.8	-	-

<sup>a</sup> The  $K_i$  values were determined in three independent experiments ( $n = 3$ ). <sup>b</sup> measured in ethanol (10  $\mu\text{M}$ ).

**In Vitro Autoradiography** *In vitro* autoradiography studies could visibly reflect the affinity of the radio-labeled tracers for  $A\beta$  plaques in brain tissue. *In vitro* autoradiography studies of the  $^{99\text{m}}\text{Tc}$ -labeled radiotracers were performed on brain sections of Tg mice (C57BL6, APPswe/PSEN1, 12-month-old, female) and age-matched control mice (C57BL6, 12-month-old, female). As shown in Figure 8 (A, C, E and G), many radioactive spots on the brain sections of Tg mice were detected, with the distribution of the  $A\beta$  plaques being identified by fluorescent staining with Thioflavin-S (Figure 8, B, D, F and H). By comparison, no radioactive accumulation was observed on the brain sections of the wild control mice (Figure S1). Although the binding affinity of  $[^{99\text{m}}\text{Tc}]\mathbf{20}$  to  $A\beta_{1-42}$  aggregates was not extremely high, the plaques in the brain sections of Tg mice was still possible with  $[^{99\text{m}}\text{Tc}]\mathbf{20}$ . In accord with the published results<sup>15</sup>,  $[^{99\text{m}}\text{Tc}]\mathbf{20} - \mathbf{23}$  displayed negative labeling of  $A\beta$  plaques on brain sections of AD patients, the reason for this may due to the different structure or conformation of  $A\beta$  plaque between Tg mouse and AD patient. However, as shown in Figure S2, they could label cerebrovascular amyloids on the brain sections of the AD patient intensely.

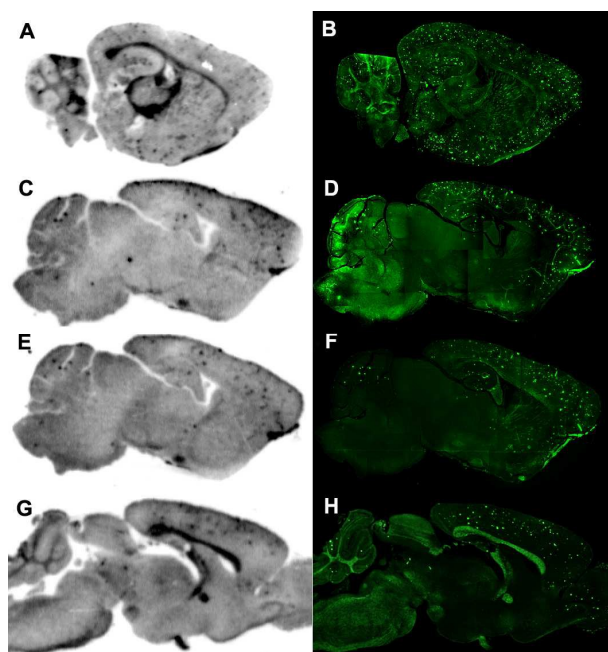


**Figure 8.** *In vitro* autoradiography of [ $^{99m}\text{Tc}$ ]20 (A), [ $^{99m}\text{Tc}$ ]21 (C), [ $^{99m}\text{Tc}$ ]22 (E) and [ $^{99m}\text{Tc}$ ]23 (G) on brain sections of Tg mice (C57BL6, APP<sup>swe</sup>/PSEN1, 12-month-old, female). The presence and distribution of A $\beta$  plaques were confirmed by fluorescence staining using Thioflavin-S on the same sections (B, D, F and H). (magnification: 5 $\times$ , DAPI filter, EX 365 nm, EM 445 nm)

***In Vivo* Biodistribution in Normal Mice** The biodistribution experiments were carried out in normal mice to evaluate the pharmacokinetics of the  $^{99m}\text{Tc}$ -labeled tracers *in vivo*, especially their ability to penetrate the BBB and their rate of washout from normal regions, which are regarded as important factors for A $\beta$  imaging probes. As shown in Table 3, [ $^{99m}\text{Tc}$ ]20 - 23 displayed unsatisfactory initial uptakes at 2 min post-injection, which were 0.50, 0.36, 0.26 and 0.37% ID/g, respectively. In addition, they possessed the property of limited clearance from the normal brain (brain<sub>2 min</sub>/brain<sub>60 min</sub> ratio is approximately 2 - 3). Although the lipophilicity of these  $^{99m}\text{Tc}$ -labeled tracers is suitable for BBB penetration, it does not offset the disadvantage that the molecular weights of these tracers are large, and some of them even exceed 600, which is considered as the maximum limit of molecular weight to cross the BBB. Furthermore, the amide bond in the linker, which could form hydrogen bonds, has a negative effect on BBB penetration. Although the [ $\text{Cp}^{99m}\text{Tc}(\text{CO})_3$ ] ligand as a lipophilic

“piano stool” organometallic core is small and neutral, the strategy that incorporated it into the 2-phenylbenzothiazole skeleton by an amide bond is not successful. Additionally, these tracers are mainly excreted by the liver and small intestine because a high accumulation of radioactivity was found in liver, and the uptake in the small intestine kept increasing after injection (Table S2).

## Conclusions

Complexes of 2-phenylbenzothiazole conjugated with [ $\text{CpM}(\text{CO})_3$ ] (M = Re,  $^{99m}\text{Tc}$ ) were successfully synthesized for the detection of A $\beta$  plaques in AD brains.  $^{99m}\text{Tc}$ -labeled tracers with high radiochemical purities have been prepared in satisfactory radiochemical yields. In *in vitro* biological evaluations, these tracers possessed optimal properties, and their sufficient binding affinities for A $\beta$  plaques and A $\beta_{1-42}$  aggregates were proven by their *in vitro* fluorescent staining of brain sections of Tg mice and an AD patient as well as in an inhibition assay. Moreover, the high specific binding of  $^{99m}\text{Tc}$ -labeled tracers to A $\beta$  plaques was verified by *in vitro* autoradiography on brain section of Tg mice. However, these tracers do not fulfill the requirements for ideal brain imaging probes because of their insufficient initial uptakes (0.26 - 0.5% ID/g) and slow clearance (the brain<sub>2 min</sub>/brain<sub>60 min</sub> ratio is approximately 2 - 3) in the brain. In summary, the preliminary results suggest that  $^{99m}\text{Tc}$ -cyclopentadienyl tricarbonyl-labeled 2-phenylbenzothiazole complexes based on the conjugate approach have some potential to detect A $\beta$  plaques in the brains of Alzheimer’s patients. However, some modifications are necessary to improve their abilities to cross the BBB and accelerate their rates of washout by additional structural refinements.

Instead of being used for radio-imaging for the detection of A $\beta$  plaques in brains, they may be used for diagnosing other diseases that are related to abnormal A $\beta$  deposits but have a low requirement for BBB penetration, such as cerebral amyloid angiopathy and cardiac amyloidosis. Moreover, it was reported that the benzothiazole skeleton possesses highly selective potent antitumor properties *in vitro* and *in vivo*; thus, the  $^{99m}\text{Tc}$ -cyclopentadienyl tricarbonyl-labeled 2-phenylbenzothiazole complexes may be developed as potential cancer radiopharmaceuticals.<sup>26, 27</sup>

**Table 3.** Brain uptake of normal mice (ICR, 5 weeks, 22 - 25 g, male) after *i.v.* injection of [ $^{99m}\text{Tc}$ ]20, [ $^{99m}\text{Tc}$ ]21, [ $^{99m}\text{Tc}$ ]22 and [ $^{99m}\text{Tc}$ ]23.

## ARTICLE

Compound	Log <i>D</i> <sup>a</sup>	Brain uptake <sup>b</sup>			
		2 min	10min	30min	60min
[ <sup>99m</sup> Tc]20	3.51 ± 0.14	0.50 ± 0.10	0.48 ± 0.09	0.28 ± 0.10	0.18 ± 0.07
[ <sup>99m</sup> Tc]21	3.17 ± 0.04	0.36 ± 0.07	0.34 ± 0.10	0.29 ± 0.08	0.19 ± 0.02
[ <sup>99m</sup> Tc]22	3.55 ± 0.10	0.26 ± 0.04	0.17 ± 0.02	0.15 ± 0.01	0.11 ± 0.02
[ <sup>99m</sup> Tc]23	3.26 ± 0.06	0.37 ± 0.08	0.12 ± 0.01	0.11 ± 0.02	0.14 ± 0.03

<sup>a</sup> Measured in triplicate with results given as the mean ± SD.

<sup>b</sup> Expressed as % injected dose per gram. Average for 5 mice ± standard deviation.

## Experimental Section

**General Information** All of the reagents used in the synthesis were commercial products and were used without further purification unless otherwise indicated. The <sup>1</sup>H-NMR and <sup>13</sup>C-NMR spectra were obtained at 400 MHz on Bruker Avance III NMR spectrometers in CDCl<sub>3</sub> and MeOD at room temperature with TMS as an internal standard. Chemical shifts were reported as δ values relative to the internal TMS. Coupling constants were reported in Hertz. Multiplicity is defined by s (singlet), d (doublet), t (triplet), and m (multiplet). Mass spectra were acquired using a SurveyorMSQ Plus (ESI) (Waltham, MA, USA) instrument. The radiochemical purity was determined by HPLC performed on a Shimadzu SCL-20 AVP system equipped with a SPD-20A UV detector (λ = 254 nm) and a Bioscan Flow Count 3200 NaI/PMT γ-radiation scintillation detector. HPLC separations and analysis were both achieved on a Venusil MP C18 reverse phase column (Agela Technologies, 5 μm, 4.6 mm × 250 mm) eluted with an isocratic system at a flow rate of 1.0 mL/min. Mobile phase A was water while mobile phase B was acetonitrile. The absorption and fluorescence spectra were measured using UV-Vis (UV-3600, Shimadzu, Japan) and fluorescence spectrophotometers (RF-5301PC, Shimadzu, Japan), respectively. Reactions were monitored by TLC (Silica gel 60 F<sub>254</sub> aluminum sheets, Merck) and visualized by illumination with a short wavelength UV lamp (λ = 254 nm or 365 nm). Column chromatography purification was performed on silica gel (54 - 74 μm) from Qingdao Haiyang Chemical Co., Ltd. Fluorescent observation was performed by the

Axio Observer Z1 inverted fluorescence microscope (Zeiss, Germany) equipped with a DAPI filter set (EX 365 nm, EM 445 nm). Normal mice (ICR, 5 weeks, 22 - 25 g, male) were used for the biodistribution experiments. All protocols requiring the use of animals were approved by the animal care committee of Beijing Normal University. Post-mortem brain tissue from autopsy-confirmed AD patients (91-year-old, male, temporal lobe) (68-year-old, female, frontal lobe) was obtained from the Chinese Brain Bank Center (CBBC) by autopsy.

## Chemistry

**Synthesis of perfluorophenyl ferrocenecarboxylate (1)** To a solution of ferrocenecarboxylic acid (231.5 mg, 1.00 mmol) in DMF (1 mL), perfluorophenyl 2,2,2-trifluoroacetate (280.4 mg, 1.00 mmol) and pyridine (150 μL) were added, and the solution was stirred at r.t. for 3 h. After the completion of the reaction, the mixture was diluted in ethyl acetate, and then it was washed by HCl (0.1 M) three times and a 5% NaHCO<sub>3</sub> solution one time. The organic layer was collected and dried over anhydrous MgSO<sub>4</sub>. Then, the organic solvent was removed in vacuum, and the residue was purified by silica gel column chromatography (column chromatography condition: petroleum ether/AcOEt = 50/1). Orange solid, 658.6 mg, yield, 56.2 %. M.p. 60.3 - 61.3 °C. <sup>1</sup>H NMR (400 MHz, CDCl<sub>3</sub>) δ 4.98 (d, *J* = 1.8 Hz, 2H), 4.59 (d, *J* = 1.9 Hz, 2H), 4.33 (s, 5H). MS (ES+): *m/z* calcd for [C<sub>17</sub>H<sub>9</sub>F<sub>5</sub>FeO<sub>2</sub>]<sup>+</sup> 396.0; found 395.8.

## ARTICLE

Compounds **4** - **7** were synthesized according to the previously reported procedure.<sup>14</sup>

**General Procedure for the Synthesis of Intermediates 8 - 11**

A solution of **4** - **7** (1 equiv) and potassium 1,3-dioxoisindolin-2-ide (2 equiv) in DMF (10 mL), under a nitrogen atmosphere, was heated at 100 °C overnight. After the completion of the reaction, DMF was removed in vacuum at 110 °C, water (20 mL) was added to the reactant after cooling, the resulting mixture was extracted by dichloromethane (3 × 20 ml) and the organic layer was dried over anhydrous MgSO<sub>4</sub>. The organic solvent was removed in vacuum, and then the residue was purified by silica gel column chromatography.

**2-(3-((2-(4-(methylamino)phenyl)benzo[d]thiazol-6-**

**yl)oxy)propyl)isoindoline-1,3-dione (8)** Yellow powder, 206.9 mg, yield, 54.9 % (column chromatography condition: petroleum ether/AcOEt/CH<sub>2</sub>Cl<sub>2</sub> = 7/1/3). M.p. 178.6 – 178.9 °C. <sup>1</sup>H NMR (400 MHz, CDCl<sub>3</sub>) δ 7.87 (d, *J* = 8.7 Hz, 2H), 7.84 (dd, *J* = 5.4, 3.1 Hz, 2H), 7.81 (d, *J* = 8.9 Hz, 1H), 7.72 (dd, *J* = 5.4, 3.0 Hz, 2H), 7.23 (d, *J* = 2.4 Hz, 1H), 6.90 (dd, *J* = 8.9, 2.5 Hz, 1H), 6.64 (d, *J* = 8.7 Hz, 2H), 4.09 (t, *J* = 6.0 Hz, 2H), 3.94 (t, *J* = 6.8 Hz, 2H), 2.91 (s, 3H), 2.26 – 2.20 (m, 2H). MS (ES<sup>+</sup>): *m/z* calcd for [C<sub>25</sub>H<sub>22</sub>N<sub>3</sub>O<sub>3</sub>S + H]<sup>+</sup> 444.1; found 443.9.

**2-(5-((2-(4-(methylamino)phenyl)benzo[d]thiazol-6-**

**yl)oxy)pentyl)isoindoline-1,3-dione (9)** Yellow powder, yield, 249.9 mg, 62.4 % (column chromatography condition: petroleum ether/AcOEt/CH<sub>2</sub>Cl<sub>2</sub> = 8/1/3). M.p. 138.8 – 139.2 °C. <sup>1</sup>H NMR (400 MHz, CDCl<sub>3</sub>) δ 7.88 (d, *J* = 8.4 Hz, 2H), 7.85 – 7.83 (m, 3H), 7.71 (dd, *J* = 5.4, 3.1 Hz, 2H), 7.28 (d, *J* = 2.4 Hz, 1H), 7.00 (dd, *J* = 8.9, 2.3 Hz, 1H), 6.65 (d, *J* = 8.6 Hz, 2H), 4.01 (t, *J* = 6.4 Hz, 2H), 3.74 (t, *J* = 7.2 Hz, 2H), 2.91 (s, 3H), 1.92 – 1.84 (m, 2H), 1.82 – 1.75 (m, 2H), 1.59 – 1.52 (m, 2H). MS (ES<sup>+</sup>): *m/z* calcd for [C<sub>27</sub>H<sub>26</sub>N<sub>3</sub>O<sub>3</sub>S + H]<sup>+</sup> 472.2; found 472.0.

**2-(3-((2-(4-(dimethylamino)phenyl)benzo[d]thiazol-6-**

**yl)oxy)propyl)isoindoline-1,3-dione (10)** Yellow powder, 555.2 mg, yield, 54.6 % (column chromatography condition: petroleum ether/AcOEt/CH<sub>2</sub>Cl<sub>2</sub> = 8/1/3). M.p. 206.8 – 207.8 °C. <sup>1</sup>H NMR (400 MHz, CDCl<sub>3</sub>) δ 7.93 (d, *J* = 8.3 Hz, 2H), 7.86 – 7.83 (m, 3H), 7.72 (dd, *J* = 5.4, 3.1 Hz, 2H), 7.23 (d, *J* = 2.4 Hz, 1H), 6.91 (dd, *J* = 8.9, 2.4 Hz, 1H), 6.76 (d, *J* = 8.6 Hz, 2H), 4.10 (t, *J* = 6.0 Hz, 2H), 3.94 (t, *J* = 6.8 Hz, 2H), 3.06 (s, 6H), 2.28 – 2.19 (m, 2H). MS (ES<sup>+</sup>): *m/z* calcd for [C<sub>26</sub>H<sub>24</sub>N<sub>3</sub>O<sub>3</sub>S + H]<sup>+</sup> 458.2; found 457.8.

**2-(5-((2-(4-(dimethylamino)phenyl)benzo[d]thiazol-6-**

**yl)oxy)pentyl)isoindoline-1,3-dione (11)** Yellow powder, 625.4 mg, yield, 87.0 % (column chromatography condition: petroleum ether/AcOEt/CH<sub>2</sub>Cl<sub>2</sub> = 7/1/3). M.p. 152.5 – 153.1 °C. <sup>1</sup>H NMR (400 MHz, CDCl<sub>3</sub>) δ 7.93 (d, *J* = 8.4 Hz, 2H), 7.88 – 7.81 (m, 3H), 7.71 (dd, *J* = 5.4, 3.1 Hz, 2H), 7.28 (d, *J* = 2.4 Hz, 1H), 7.00 (dd, *J* = 8.9, 2.4 Hz, 1H), 6.75 (d, *J* = 8.8 Hz, 2H), 4.01 (t, *J* = 6.4 Hz, 2H), 3.74 (t, *J* = 7.2 Hz, 2H), 3.05 (s, 6H), 1.91 – 1.84 (m, 2H), 1.79 – 1.75 (m, 2H), 1.60 – 1.52 (m, 2H). MS (ES<sup>+</sup>): *m/z* calcd for [C<sub>28</sub>H<sub>28</sub>N<sub>3</sub>O<sub>3</sub>S + H]<sup>+</sup> 486.2; found 485.9.

**General Procedure for the Synthesis of Intermediates 12 - 15**

A solution of **8** - **11** (1 equiv) and hydrazine hydrate (10 equiv) was heated for 2 h at 100 °C in EtOH (20 mL). After the yellow suspension turned white, the solvent was removed in vacuum and water was added. The resulting mixture was extracted by dichloromethane (3 × 20 ml), and the organic layer was dried over anhydrous MgSO<sub>4</sub>. The organic solvent was removed in vacuum, and then the residue was purified by silica gel column chromatography or recrystallization.

**4-(6-(3-aminopropoxy)benzo[d]thiazol-2-yl)-N-methylaniline**

**(12)** White powder, 185 mg, yield, 65.6 % (recrystallization condition: petroleum ether/AcOEt = 5/1). M.p. 107.3 – 108.1 °C. <sup>1</sup>H NMR (400 MHz, CDCl<sub>3</sub>) δ 7.88 – 7.84 (m, 3H), 7.32 (d, *J* = 2.4 Hz, 1H), 7.03 (dd, *J* = 8.9, 2.5 Hz, 1H), 6.64 (d, *J* = 8.7 Hz, 2H), 4.12 (t, *J* = 6.1 Hz, 2H), 2.94 (t, *J* = 6.8 Hz, 2H), 2.91 (s, 3H), 2.00 – 1.94 (m, 2H). MS (ES<sup>+</sup>): *m/z* calcd for [C<sub>17</sub>H<sub>20</sub>N<sub>3</sub>OS + H]<sup>+</sup> 314.1; found 314.1.

**4-(6-((5-aminopentyl)oxy)benzo[d]thiazol-2-yl)-N-methylaniline**

**(13)** White powder, 206.9 mg, yield, 63.8 % (column chromatography condition: AcOEt/CH<sub>2</sub>Cl<sub>2</sub>/CH<sub>3</sub>OH = 5/5/3). M.p. 85.6 – 86.3 °C. <sup>1</sup>H NMR (400 MHz, CDCl<sub>3</sub>) δ 7.93 – 7.78 (m, 3H), 7.30 (s, 1H), 7.02 (dd, *J* = 8.9, 2.0 Hz, 1H), 6.64 (d, *J* = 8.6 Hz, 2H), 4.02 (t, *J* = 6.4 Hz, 2H), 2.91 (s, 3H), 2.75 (t, *J* = 6.5 Hz, 2H), 1.88 – 1.81 (m, 2H), 1.63 – 1.43 (m, 4H). MS (ES<sup>+</sup>): *m/z* calcd for [C<sub>19</sub>H<sub>24</sub>N<sub>3</sub>OS + H]<sup>+</sup> 342.2; found 342.0.

**4-(6-(3-aminopropoxy)benzo[d]thiazol-2-yl)-N,N-dimethylaniline**

**(14)** White powder, 175.0 mg, yield, 96.4 % (recrystallization condition: petroleum ether/AcOEt = 5/1). M.p. 147.4 – 148.1 °C. <sup>1</sup>H NMR (400 MHz, CDCl<sub>3</sub>) δ 7.90 (d, *J* = 8.9 Hz, 2H), 7.85 (d, *J* = 8.9 Hz, 2H), 7.32 (d, *J* = 2.5 Hz, 1H), 7.03 (dd, *J* = 8.9, 2.5 Hz, 1H), 6.74 (d, *J* = 8.9 Hz, 2H), 4.12 (t, *J* = 6.1 Hz, 2H), 3.05 (s, 6H), 2.94

## Journal Name

(t,  $J = 6.7$  Hz, 2H), 2.00 – 1.92 (m, 2H). MS (ES<sup>+</sup>):  $m/z$  calcd for  $[C_{18}H_{22}N_3OS + H]^+$  328.1; found 328.0.

**4-(6-((5-aminopentyl)oxy)benzo[d]thiazol-2-yl)-N,N-**

**dimethylaniline (15)** White powder, 366.4 mg, yield, 83.1 % (column chromatography condition: petroleum ether/CH<sub>2</sub>Cl<sub>2</sub>/CH<sub>3</sub>OH/Et<sub>3</sub>N = 30/10/1/1). M.p. 101.2 – 102.4 °C. <sup>1</sup>H NMR (400 MHz, CDCl<sub>3</sub>)  $\delta$  7.90 (d,  $J = 8.9$  Hz, 2H), 7.85 (d,  $J = 8.9$  Hz, 1H), 7.30 (d,  $J = 2.4$  Hz, 1H), 7.02 (dd,  $J = 8.9, 2.5$  Hz, 1H), 6.74 (d,  $J = 8.9$  Hz, 2H), 4.03 (t,  $J = 6.4$  Hz, 2H), 3.05 (s, 6H), 2.74 (t,  $J = 6.4$  Hz, 2H), 1.88 – 1.80 (m, 2H), 1.56 – 1.52 (m, 4H). MS (ES<sup>+</sup>):  $m/z$  calcd for  $[C_{20}H_{26}N_3OS + H]^+$  356.2; found 356.1.

**General Procedure for the Synthesis of Ferrocene Precursors 16 - 19**

To a stirring solution of **11** - **15** (1 equiv) in anhydrous DMF, compound **1** (1 equiv) and triethylamine (150  $\mu$ L) were added. The resulting mixture was stirred for 4 h at room temperature, and then the solvent was removed under reduced pressure. The residue was purified by silica gel column chromatography.

**N-(3-((2-(4-(methylamino)phenyl)benzo[d]thiazol-6-**

**yl)oxy)propyl)carboxamide)-ferrocene (16)** Orange powder, 189.2 mg, yield, 72.3 % (column chromatography condition: petroleum ether/AcOEt/CH<sub>2</sub>Cl<sub>2</sub> = 2/1/1). M.p. 227.7 – 229.2 °C. <sup>1</sup>H NMR (400 MHz, CDCl<sub>3</sub>)  $\delta$  7.95 – 7.70 (m, 3H), 7.36 (d,  $J = 1.9$  Hz, 1H), 7.09 (dd,  $J = 8.8, 1.8$  Hz, 1H), 6.66 (d,  $J = 8.5$  Hz, 2H), 6.16 (s, 1H), 4.67 (s, 2H), 4.35 (s, 2H), 4.21 – 4.13 (m, 7H), 3.66 – 3.61 (m, 2H), 2.92 (s, 3H), 2.19 – 2.10 (m, 2H). MS (ES<sup>+</sup>):  $m/z$  calcd for  $[C_{28}H_{28}FeN_3O_2S + H]^+$  526.1; found 526.0.

**N-(5-((2-(4-(methylamino)phenyl)benzo[d]thiazol-6-**

**yl)oxy)pentyl)carboxamide)-ferrocene (17)** Orange powder, 179.4 mg, yield, 54.0 % (column chromatography condition: petroleum ether/AcOEt/CH<sub>2</sub>Cl<sub>2</sub> = 2/1/1). M.p. 198.5 – 199.7 °C. <sup>1</sup>H NMR (400 MHz, CDCl<sub>3</sub>)  $\delta$  7.91 – 7.89 (m, 3H), 7.30 (s, 1H), 7.03 (d,  $J = 8.7$  Hz, 1H), 6.65 (d,  $J = 8.1$  Hz, 2H), 5.72 (s, 1H), 4.65 (s, 2H), 4.33 (s, 2H), 4.20 (s, 5H), 4.05 (t,  $J = 6.0$  Hz, 2H), 3.46 – 3.39 (m, 2H), 2.91 (s, 3H), 1.93 – 1.89 (m, 2H), 1.73 – 1.68 (m, 2H), 1.66 – 1.57 (m, 2H). MS (ES<sup>+</sup>):  $m/z$  calcd for  $[C_{30}H_{32}FeN_3O_2S + H]^+$  554.2; found 554.0.

**N-(3-((2-(4-(dimethylamino)phenyl)benzo[d]thiazol-6-**

**yl)oxy)propyl)carboxamide)-ferrocene (18)** Orange powder, 22.5 mg, yield, 41.7 % (column chromatography condition: petroleum

ether/AcOEt/CH<sub>2</sub>Cl<sub>2</sub> = 3/1/1). M.p. 219.4 – 220.1 °C. <sup>1</sup>H NMR (400 MHz, CDCl<sub>3</sub>)  $\delta$  7.97 – 7.95 (m, 3H), 7.36 (d,  $J = 1.7$  Hz, 1H), 7.10 (dd,  $J = 8.9, 2.2$  Hz, 1H), 6.77 (d,  $J = 8.6$  Hz, 2H), 6.14 (s, 2H), 4.67 (s, 2H), 4.35 (s, 2H), 4.22 – 4.15 (m, 7H), 3.68 – 3.60 (m, 2H), 3.07 (s, 6H), 2.18 – 2.11 (m, 2H). MS (ES<sup>+</sup>):  $m/z$  calcd for  $[C_{29}H_{30}FeN_3O_2S + H]^+$  540.1; found 539.9.

**N-(5-((2-(4-(dimethylamino)phenyl)benzo[d]thiazol-6-**

**yl)oxy)pentyl)carboxamide)-ferrocene (19)** Orange powder, 239.4 mg, yield, 84.4 % (column chromatography condition: petroleum ether/AcOEt/CH<sub>2</sub>Cl<sub>2</sub> = 3/1/1). M.p. 189.0 – 189.4 °C. <sup>1</sup>H NMR (400 MHz, CDCl<sub>3</sub>)  $\delta$  7.91 (d,  $J = 8.6$  Hz, 2H), 7.86 (d,  $J = 8.7$  Hz, 1H), 7.30 (t,  $J = 7.0$  Hz, 1H), 7.03 (dd,  $J = 8.9, 2.4$  Hz, 1H), 6.75 (d,  $J = 8.8$  Hz, 2H), 5.70 (s, 1H), 4.65 (s, 2H), 4.33 (s, 2H), 4.20 (s, 5H), 4.05 (t,  $J = 6.2$  Hz, 2H), 3.45 – 3.40 (m, 2H), 3.05 (s, 6H), 1.91 – 1.87 (m, 2H), 1.71 – 1.66 (m, 2H), 1.65 – 1.58 (m, 2H). MS (ES<sup>+</sup>):  $m/z$  calcd for  $[C_{31}H_{34}FeN_3O_2S + H]^+$  568.2; found 568.0.

**General Procedure for the Synthesis of Rhenium Complexes 20 – 23**

A solution of  $[Re(CO)_3Cl_3][NEt_4]_2$  (1.5 equiv) and **16** - **19** (1 equiv) in DMF (2.5 ml) and 0.5 ml of HCl (1 M) were sealed in an autoclave with a magnetic stir bar at 160 °C for 2 h. After cooling, the reaction mixture was poured into a dichloromethane solution (10 ml). The solvent was removed in vacuum, and the crude product was purified by column chromatography on silica gel.

**N-(3-((2-(4-(methylamino)phenyl)benzo[d]thiazol-6-****yl)oxy)propyl)carboxamide)-**

**(cyclopentadienyl)tricarbonylrhenium (20)** Light yellow powder, 18.3 mg, yield, 27.0 % (column chromatography condition: petroleum ether/CH<sub>2</sub>Cl<sub>2</sub> = 1/1 (containing 5% of Et<sub>3</sub>N)). M.p. 181.7 – 183.0 °C. <sup>1</sup>H NMR (400 MHz, CDCl<sub>3</sub>)  $\delta$  7.90 – 7.86 (m, 3H), 7.31 (d,  $J = 1.8$  Hz, 1H), 7.02 (dd,  $J = 8.9, 2.0$  Hz, 1H), 6.65 (d,  $J = 8.5$  Hz, 2H), 6.29 (s, 1H), 5.87 (s, 2H), 5.36 (s, 2H), 4.14 (t,  $J = 5.5$  Hz, 2H), 3.62 – 3.58 (m, 2H), 2.92 (s, 3H), 2.12 – 2.01 (m, 2H). <sup>13</sup>C NMR (100 MHz, CDCl<sub>3</sub>)  $\delta$  192.44, 166.87, 162.23, 156.00, 151.36, 149.22, 135.94, 128.81, 122.95, 122.68, 115.30, 112.08, 105.38, 95.49, 85.38, 84.90, 67.31, 37.99, 30.37, 28.79, 26.93. TOF MS (ES<sup>+</sup>):  $m/z$  calcd for  $[C_{26}H_{23}N_3O_5S^{185}Re + H]^+$  674.0888; found 674.0892.

**N-(5-((2-(4-(methylamino)phenyl)benzo[d]thiazol-6-****yl)oxy)pentyl)carboxamide)-**

**(cyclopentadienyl)tricarbonylrhenium (21)** Light yellow powder,

## ARTICLE

18.5 mg, yield, 26.3 % (column chromatography condition: petroleum ether /CH<sub>2</sub>Cl<sub>2</sub> = 1/1 (containing 5% of Et<sub>3</sub>N)). M.p. 189.3 – 190.1 °C. <sup>1</sup>H NMR (400 MHz, CDCl<sub>3</sub>) δ 7.91 – 7.89 (m, 3H), 7.28 (s, 1H), 7.03 (d, *J* = 8.9 Hz, 1H), 6.66 (d, *J* = 8.5 Hz, 2H), 5.87 (s, 2H), 5.75 (s, 1H), 5.35 (s, 2H), 4.02 (t, *J* = 6.1 Hz, 2H), 3.44 – 3.34 (m, 2H), 2.92 (s, 3H), 1.87 – 1.83 (m, 2H), 1.68 – 1.64 (m, 2H), 1.59 – 1.53 (m, 2H). <sup>13</sup>C NMR (100 MHz, CDCl<sub>3</sub>) δ 192.48, 169.92, 167.00, 162.20, 156.77, 150.89, 134.81, 129.07, 122.47, 118.48, 115.72, 112.25, 105.23, 95.37, 85.67, 84.77, 68.38, 39.73, 30.40, 29.28, 28.84, 23.47. TOF MS (ES<sup>+</sup>): *m/z* calcd for [C<sub>28</sub>H<sub>27</sub>N<sub>3</sub>O<sub>5</sub>S<sup>185</sup>Re + H]<sup>+</sup> 702.1201; found 702.1219.

**N-(3-((2-(4-(dimethylamino)phenyl)benzo[d]thiazol-6-yl)oxy)propyl)carboxamide)-**

**(cyclopentadienyl)tricarbonylrhenium (22)** Light yellow powder, 24.7 mg, yield, 35.9 % (column chromatography condition: petroleum ether /CH<sub>2</sub>Cl<sub>2</sub> = 1/1 (containing 2% of Et<sub>3</sub>N)). M.p. 171.6 – 172.1 °C. <sup>1</sup>H NMR (400 MHz, CDCl<sub>3</sub>) δ 7.91 (d, *J* = 8.8 Hz, 2H), 7.86 (d, *J* = 8.9 Hz, 1H), 7.30 (d, *J* = 2.4 Hz, 1H), 7.01 (dd, *J* = 8.9, 2.5 Hz, 1H), 6.74 (d, *J* = 8.9 Hz, 2H), 6.34 (s, 1H), 5.86 (s, 2H), 5.36 – 5.35 (m, 2H), 4.13 (t, *J* = 5.6 Hz, 2H), 3.61 – 3.57 (m, 2H), 3.06 (s, 6H), 2.12 – 2.06 (m, 2H). <sup>13</sup>C NMR (100 MHz, CDCl<sub>3</sub>) δ 192.49, 166.98, 162.28, 156.05, 152.10, 148.88, 135.68, 128.66, 122.69, 121.22, 115.36, 111.81, 105.38, 95.48, 85.47, 84.92, 67.19, 40.21, 37.86, 28.79, 26.93. TOF MS (ES<sup>+</sup>): *m/z* calcd for [C<sub>27</sub>H<sub>25</sub>N<sub>3</sub>O<sub>5</sub>S<sup>185</sup>Re + H]<sup>+</sup> 688.1045; found 688.1060.

**N-(5-((2-(4-(dimethylamino)phenyl)benzo[d]thiazol-6-yl)oxy)pentyl)carboxamide)-**

**(cyclopentadienyl)tricarbonylrhenium (23)** Light yellow powder, 23.2 mg, yield, 32.4 % (column chromatography condition: petroleum ether /CH<sub>2</sub>Cl<sub>2</sub> = 1/1 (containing 2% of Et<sub>3</sub>N)). M.p. 149.1 – 150.1 °C. <sup>1</sup>H NMR (400 MHz, CDCl<sub>3</sub>) δ 7.96 – 7.90 (m, 3H), 7.29 (s, 1H), 7.03 (d, *J* = 8.7 Hz, 1H), 6.76 (d, *J* = 8.4 Hz, 2H), 5.87 (s, 2H), 5.75 (s, 1H), 5.35 (s, 2H), 4.02 (t, *J* = 5.9 Hz, 2H), 3.44 – 3.36 (m, 2H), 3.06 (s, 6H), 1.89 – 1.82 (m, 2H), 1.69 – 1.65 (m, 2H), 1.62 – 1.52 (m, 2H). <sup>13</sup>C NMR (100 MHz, MeOD) δ 194.23, 168.72, 164.76, 158.34, 153.79, 149.38, 136.65, 129.43, 123.05, 122.10, 116.90, 112.94, 106.20, 96.01, 87.77, 86.47, 70.81, 43.86, 40.48, 40.28, 30.20, 30.06, 24.53. TOF MS (ES<sup>+</sup>): *m/z* calcd for [C<sub>29</sub>H<sub>29</sub>N<sub>3</sub>O<sub>5</sub>S<sup>185</sup>Re + H]<sup>+</sup> 716.1358; found 716.1364.

**X-ray Crystallography** Single-crystal X-ray diffraction measurements were performed on a Bruker Smart APEXII CCD

diffractometer at 100 K using graphite monochromated Mo K $\alpha$  radiation ( $\lambda$  = 0.71073 Å). The structures were solved by direct methods and refined by a full-matrix least-squares on *F*<sup>2</sup> using the SHELXL-97 program package.<sup>28</sup>

**Preparation of [<sup>99m</sup>Tc]20, [<sup>99m</sup>Tc]21, [<sup>99m</sup>Tc]22 and [<sup>99m</sup>Tc]23**

To a solution of ferrocene precursor (1.0 mg) and Mn(CO)<sub>5</sub>Br (1.0 mg) in DMF (0.7 mL), a Na[<sup>99m</sup>TcO<sub>4</sub>] aqueous solution (370 MBq, 1.0 mL) was added. The reaction mixture was heated at 150 °C for 50 min in a sealed vial. After cooling, the mixture was extracted by CH<sub>2</sub>Cl<sub>2</sub>, the organic solvent was collected and removed under a stream of nitrogen gas, the residue was dissolved in CH<sub>3</sub>CN and it was purified by radio-HPLC under the following conditions: Venusil MP C18 column (Agela Technologies, 4.6 mm × 250 mm), CH<sub>3</sub>CN/H<sub>2</sub>O = 65/35 for [<sup>99m</sup>Tc]20, CH<sub>3</sub>CN/H<sub>2</sub>O = 70/30 for [<sup>99m</sup>Tc]21, [<sup>99m</sup>Tc]22, and [<sup>99m</sup>Tc]23, 1 mL/min, UV = 254 nm. The <sup>99m</sup>Tc-labeled tracers were confirmed by comparative HPLC using the corresponding rhenium surrogates.

**Partition Coefficient Determination** The partition coefficients of the <sup>99m</sup>Tc-labeled complexes were determined according to the previously reported procedure.<sup>18</sup>

**In Vitro Fluorescent Staining** The brain sections of Tg mice (C57BL6, APP<sup>swe</sup>/PSEN1, 12-month-old, female) and the post-mortem brain tissues from an autopsy-confirmed case of AD (91-year-old, male, temporal lobe) were deparaffinized with soaking in xylene for 5 min and then 100% ethanol for 5 min. The brain sections were incubated with 25% ethanol solutions (1.0 μM) of rhenium complexes **20**, **21**, **22** and **23** for 10 min as well as Thioflavin-S (0.125%), which was used for comparison to stain the adjacent sections. Then, the sections were washed by 40% ethanol for 5 min. Fluorescent observation was carried out by an Axio Observer Z1 (Zeiss, Germany) equipped with DAPI filter set (EX 365 nm, EM 445 nm).

**In Vitro Inhibition Assay** Inhibition experiments were performed in borosilicate glass tubes (12 mm × 75 mm) according to previously described procedures with some modifications.<sup>14</sup> One hundred microliters of A $\beta$  aggregated fibrils (28 nM in the final assay mixture) was added to a mixture that contained 100 μL of radioligand ([<sup>125</sup>I]IMPY, prepared as reported previously, 100000 cpm/100 μL), 100 μL of inhibitor (complexes **20**, **21**, **22** and **23**, 10<sup>-4</sup> M to 10<sup>-9.5</sup> M in ethanol), 100 μL of DMSO and 600 μL of BSA (0.1 %, pH = 7.4) in a final volume of 1.0 mL. Then, incubation,

## Journal Name

separation and data processing were carried out as previously reported.

**In Vitro Autoradiography** Paraffin-embedded brain sections of Tg (C57BL6, APP<sup>sw</sup>/PSEN1, 12-month-old, female), control mice (C57BL6, 12-month-old, female) and an AD patient (68-year-old, female, frontal lobe) were disposed according to the method in the *in vitro* fluorescent staining experiment. Then, the sections were incubated with [<sup>99m</sup>Tc]20, [<sup>99m</sup>Tc]21, [<sup>99m</sup>Tc]22 and [<sup>99m</sup>Tc]23, ( $3.7 \times 10^6$  Bq/100  $\mu$ L) for 1 h at room temperature. They were washed with 40% EtOH for 5 min. The sections were dried and placed in a phosphorus plate (Perkin-Elmer, USA) for another 1 h. *In vitro* autoradiographic images were visualized using a phosphor imaging system (Cyclone, Packard). Thereafter, the distribution of A $\beta$  plaques in the same brain sections was confirmed by staining with Thioflavin-S according to the method in the *in vitro* fluorescent staining experiment.

**In Vivo Biodistribution Studies** A saline solution containing purified <sup>99m</sup>Tc-labeled tracers (100  $\mu$ L, 10% ethanol, 185 KBq) was injected via the tail vein of normal mice (ICR, 5 weeks, 22 - 25 g, male). The mice were sacrificed at exact various time points post-injection (2, 10, 30 and 60 min). Samples of blood and interesting organs were obtained, weighed, and the radioactivity was measured with an automatic  $\gamma$ -counter.

### Acknowledgements

The authors present special thanks to Dr. Jin Liu (College of Life Science, Beijing Normal University) for assistance in the *in vitro* fluorescent staining. This work was funded by the National Natural Science Foundation of China (No. 21201019) and the Beijing Municipal Natural Science Foundation (No. 7143180).

### Notes and references

<sup>a</sup> Key Laboratory of Radiopharmaceuticals, Ministry of Education, College of Chemistry, Beijing Normal University, Beijing 100875, P. R. China.

<sup>b</sup> Wuhan Institute for Neuroscience and Neuroengineering, South-Central University for Nationalities, Wuhan 430074, P. R. China.

\* Corresponding author, email: cmc@bnu.edu.cn

Electronic Supplementary Information (ESI) available: *In vitro* and *in vivo* evaluations are presented including four figures and two tables as described in the text, as well as spectrograms of all synthesized complexes. See DOI: 10.1039/b000000x/

1. Karran, E.; Mercken, M.; De Strooper, B. The amyloid cascade hypothesis for Alzheimer's disease: an appraisal for the development of therapeutics. *Nat. Rev. Drug Discovery* **2011**, *10*, 698-712.
2. Mucke, L. Neuroscience: Alzheimer's disease. *Nature* **2009**, *461*, 895-897.
3. Hardy, J.; Selkoe, D. J. The amyloid hypothesis of Alzheimer's disease: progress and problems on the road to therapeutics. *Science* **2002**, *297*, 353-356.
4. Binder, L. I.; Guillozet-Bongaarts, A. L.; Garcia-Sierra, F.; Berry, R. W. Tau, tangles, and Alzheimer's disease. *Biochim. Biophys. Acta, Mol. Basis Dis.* **2005**, *1739*, 216-223.
5. Clark, C. M.; Schneider, J. A.; Bedell, B. J.; Beach, T. G.; Bilker, W. B.; Mintun, M. A.; Pontecorvo, M. J.; Hefti, F.; Carpenter, A. P.; Flitter, M. L. Use of florbetapir-PET for imaging  $\beta$ -amyloid pathology. *J. Am. Med. Assoc.* **2011**, *305*, 275-283.
6. Sperling, R. A.; Johnson, K. A.; Doraiswamy, P. M.; Reiman, E. M.; Fleisher, A. S.; Sabbagh, M. N.; Sadowsky, C. H.; Carpenter, A.; Davis, M. D.; Lu, M. Amyloid deposition detected with florbetapir F 18 (<sup>18</sup>F-AV-45) is related to lower episodic memory performance in clinically normal older individuals. *Neurobiol. Aging* **2013**, *34*, 822-831.
7. Wong, D. F.; Moghekar, A. R.; Rigamonti, D.; Brašić, J. R.; Rousset, O.; Willis, W.; Buckley, C.; Smith, A.; Gok, B.; Sherwin, P. An *in vivo* evaluation of cerebral cortical amyloid with [<sup>18</sup>F] flutemetamol using positron emission tomography compared with parietal biopsy samples in living normal pressure hydrocephalus patients. *Mol. Imaging Biol.* **2013**, *15*, 230-237.
8. Wolk, D. A.; Grachev, I. D.; Buckley, C.; Kazi, H.; Grady, M. S.; Trojanowski, J. Q.; Hamilton, R. H.; Sherwin, P.; McLain, R.; Arnold, S. E. Association between *in vivo* fluorine 18-labeled flutemetamol amyloid positron emission tomography imaging and *in vivo* cerebral cortical histopathology. *Arch. Neurol.* **2011**, *68*, 1398-1403.
9. Barthel, H.; Sabri, O. Florbetaben to trace amyloid- $\beta$  in the Alzheimer brain by means of PET. *J. Alzheimers Dis.* **2011**, *26*, 117-121.
10. Fodero-Tavoletti, M. T.; Brockschneider, D.; Villemagne, V. L.; Martin, L.; Connor, A. R.; Thiele, A.; Berndt, M.; McLean, C. A.; Krause, S.; Rowe, C. C. *In vitro* characterization of [<sup>18</sup>F]-

## ARTICLE

- florbetaben, an  $A\beta$  imaging radiotracer. *Nucl. Med. Biol.* **2012**, *39*, 1042-1048.
11. Chen, X.; Yu, P.; Zhang, L.; Liu, B. Synthesis and biological evaluation of  $^{99m}\text{Tc}$ , Re-monoamine-monoamide conjugated to 2-(4-aminophenyl) benzothiazole as potential probes for  $\beta$ -amyloid plaques in the brain. *Bioorg. Med. Chem. Lett.* **2008**, *18*, 1442-1445.
12. Serdons, K.; Verduyck, T.; Cleynhens, J.; Bormans, G.; Verbruggen, A. Development of  $^{99m}\text{Tc}$ -thioflavin-T derivatives for detection of systemic amyloidosis. *J. Labelled Compd. Radiopharm.* **2008**, *51*, 357-367.
13. Sagnou, M.; Tzanopoulou, S.; Raptopoulou, C. P.; Psycharis, V.; Braband, H.; Alberto, R.; Pirmettis, I. C.; Papadopoulos, M.; Pelecanou, M. A phenylbenzothiazole conjugate with the tricarbonyl fac-[M(I)(CO) $_3$ ] $^+$  (M = Re,  $^{99}\text{Tc}$ ,  $^{99m}\text{Tc}$ ) core for imaging of  $\beta$ -amyloid plaques. *Eur. J. Inorg. Chem.* **2012**, *2012*, 4279-4286.
14. Jia, J.; Cui, M.; Dai, J.; Wang, X.; Ding, Y.-S.; Jia, H.; Liu, B.  $^{99m}\text{Tc}$ -labeled benzothiazole and stilbene derivatives as imaging agents for  $A\beta$  plaques in cerebral amyloid angiopathy. *Med. Chem. Comm.* **2014**, *5*, 153-158.
15. Zhuang, Z.; Kung, M.; Hou, C.; Ploessl, K.; Kung, H. Biphenyls labeled with technetium 99m for imaging beta-amyloid plaques in the brain. *Nucl. Med. Biol.* **2005**, *32*, 171-84.
16. Ono, M.; Ikeoka, R.; Watanabe, H.; Kimura, H.; Fuchigami, T.; Haratake, M.; Saji, H.; Nakayama, M.  $^{99m}\text{Tc}$ /Re complexes based on flavone and aurone as SPECT probes for imaging cerebral  $\beta$ -amyloid plaques. *Bioorg. Med. Chem. Lett.* **2010**, *20*, 5743-5748.
17. Yang, Y.; Zhu, L.; Cui, M.; Tang, R.; Zhang, H. Preparation of classical  $\text{Re}^{99m}\text{Tc}(\text{CO})_3^+$  and novel  $^{99m}\text{Tc}(\text{CO})_2(\text{NO})_2^+$  cores complexed with flavonol derivatives and their binding characteristics for A $\beta$  (1-40) aggregates. *Bioorg. Med. Chem. Lett.* **2010**, *20*, 5337-5344.
18. Li, Z.; Cui, M.; Dai, J.; Wang, X.; Yu, P.; Yang, Y.; Jia, J.; Fu, H.; Ono, M.; Jia, H. Novel cyclopentadienyl tricarbonyl complexes of  $^{99m}\text{Tc}$  mimicking chalcone as potential single-photon emission computed tomography imaging probes for  $\beta$ -Amyloid plaques in brain. *J. Med. Chem.* **2013**, *56*, 471-482.
19. Ono, M.; Ikeoka, R.; Watanabe, H.; Kimura, H.; Fuchigami, T.; Haratake, M.; Saji, H.; Nakayama, M. Synthesis and evaluation of novel chalcone derivatives with  $^{99m}\text{Tc}$ /Re complexes as potential probes for detection of  $\beta$ -amyloid plaques. *ACS Chem. Neurosci.* **2010**, *1*, 598-607.
20. Cheng, Y.; Ono, M.; Kimura, H.; Ueda, M.; Saji, H. Technetium-99m labeled pyridyl benzofuran derivatives as single photon emission computed tomography imaging probes for  $\beta$ -amyloid plaques in Alzheimer's brains. *J. Med. Chem.* **2012**, *55*, 2279-2286.
21. Bernard, J.; Ortner, K.; Spingler, B.; Pietzsch, H.J.; Alberto, R. Aqueous synthesis of derivatized cyclopentadienyl complexes of technetium and rhenium directed toward radiopharmaceutical application. *Inorg. Chem.* **2003**, *42*, 1014-1022.
22. Saidi, M.; Seifert, S.; Kretzschmar, M.; Bergmann, R.; Pietzsch, H.-J. Cyclopentadienyl tricarbonyl complexes of  $^{99m}\text{Tc}$  for the in vivo imaging of the serotonin 5-HT $_{1A}$  receptor in the brain. *J. Organomet. Chem.* **2004**, *689*, 4739-4744.
23. Saidi, M.; Kothari, K.; Pillai, M.; Hassan, A.; Sarma, H.; Chaudhari, P.; Unnikrishnan, T.; Korde, A.; Azzouz, Z. Cyclopentadienyl technetium ( $^{99m}\text{Tc}$ ) tricarbonyl piperidine conjugates: biodistribution and imaging studies. *J. Labelled Compd. Radiopharm.* **2001**, *44*, 603-618.
24. Cui, M.; Wang, X.; Yu, P.; Zhang, J.; Li, Z.; Zhang, X.; Yang, Y.; Ono, M.; Jia, H.; Saji, H. Synthesis and evaluation of novel  $^{18}\text{F}$  labeled 2-pyridinylbenzoxazole and 2-pyridinylbenzothiazole derivatives as ligands for positron emission tomography (PET) imaging of  $\beta$ -amyloid plaques. *J. Med. Chem.* **2012**, *55*, 9283-9296.
25. Cui, M. Past and recent progress of molecular imaging probes for  $\beta$ -Amyloid plaques in the brain. *Curr. Med. Chem.* **2014**, *21*, 82-112.
26. Chua, M.-S.; Kashiwayama, E.; Bradshaw, T. D.; Stinson, S. F.; Brantley, E.; Sausville, E. A.; Stevens, M. F. Role of CYP1A1 in modulation of antitumor properties of the novel agent 2-(4-amino-3-methylphenyl) benzothiazole (DF 203, NSC 674495) in human breast cancer cells. *Cancer Res.* **2000**, *60*, 5196-5203.
27. Tzanopoulou, S.; Pirmettis, I. C.; Patsis, G.; Paravatou-Petsotas, M.; Livaniou, E.; Papadopoulos, M.; Pelecanou, M. Synthesis, characterization, and biological evaluation of M(I)(CO) $_3$ (NNO) complexes (M = Re,  $^{99m}\text{Tc}$ ) conjugated to 2-(4-aminophenyl) benzothiazole as potential breast cancer radiopharmaceuticals. *J. Med. Chem.* **2006**, *49*, 5408-5410.
28. Sheldrick, G. SHELXS-97, program for X-ray crystal structure determination. *Göttingen University, Germany* **1997**.

**Conjugate approach**

Affinity to A $\beta_{1-42}$ aggregates	
Compound	$K_i$ (nM)
<b>20</b>	142.6 $\pm$ 29.5
<b>21</b>	75.8 $\pm$ 36.3
<b>22</b>	64.1 $\pm$ 13.9
<b>23</b>	24.0 $\pm$ 8.1
<b>IMPY</b>	12.5 $\pm$ 2.8

**20** n = 3, R = H, M = Re; [<sup>99m</sup>Tc]**20** M = <sup>99m</sup>Tc  
**21** n = 5, R = H, M = Re; [<sup>99m</sup>Tc]**21** M = <sup>99m</sup>Tc  
**22** n = 3, R = Me, M = Re; [<sup>99m</sup>Tc]**22** M = <sup>99m</sup>Tc  
**23** n = 5, R = Me, M = Re; [<sup>99m</sup>Tc]**23** M = <sup>99m</sup>Tc

[CpM(CO)<sub>3</sub>] (M = Re, <sup>99m</sup>Tc) labeled 2-Phenylbenzothiazoles designed by conjugate approach were evaluated as SPECT tracers for A $\beta$  plaques.

423x147mm (72 x 72 DPI)